ISET Journal of Earthquake Technology, Paper No. 588, Vol. 61, No. 3, Sept. 2024, pp. 91–106

ANALYSIS OF ACTIVE TECTONIC DEFORMATION OF TUPUL WATERSHED MANIPUR, INDIA: INFERENCES FROM RIVER PROFILE AND OTHER MORPHOMETRIC PARAMETERS

Yumkhaibam Sanjitkumar Singh (Corresponding Author)
Department of Earth Sciences, Manipur University
Imphal-795003, India, E mail id: ysksingh@gmail.com

Yumkhaibam Rajesh Singh
Department of Earth Sciences, Manipur University
Imphal-795003, India, E mail id: yumkhaibam.rajesh@manipuruniv.ac.in

Manichandra Sanoujam
Seismological Observatory, Department of Earth Sciences, Manipur University
Imphal-795003, India, E mail id: mcsanoujam@gmail.com

ABSTRACT

The study evaluates the tectonic activity of the Tupul basin in Manipur, spanning parts of Noney, Kangpokpi, and Churachandpur districts. Data from DEM, SENTINEL-2 satellite imagery, SOI-toposheets, and field verification were used to analyze geomorphic indices such as the *SL* index, Transverse Topographic Symmetry (*T*), Valley Floor Width to valley Height ratio (V_f), Drainage Basin Asymmetry (*AF*), and Basin Elongation Ratio (E_b), along with hypsometric curve and integral calculations. The findings highlight significant tectonic influences. *SL* index values (>10) identify knick points, while a *T*-value of 0.422 indicates basin asymmetry. V_f ratios (0.085–0.186) suggest active incision forming V-shaped valleys. An *AF* of 70.32% reveals northeastern uplift causing river shifts southwest, and E_b value of 0.64 indicates tectonic deformation. The hypsometric integral (49.5%) suggests the basin is in an early mature erosion stage. The 101.0 km² basin demonstrates active tectonic uplift, erosion, and river adjustments.

KEYWORDS: Morphotectonic indices, active tectonics, geology, drainage basin, hypsometry

INTRODUCTION

The study of landforms and tectonic activity in a given area involves the precise calculation of various geomorphic indices. These indices, derived from satellite data, topographic maps, and aerial photographs, provide valuable insights into the tectonic history and dynamics of the region (Keller 1986). By adopting a multidisciplinary approach that incorporates geomorphological, structural, and neotectonic analyses, researchers can evaluate active tectonics comprehensively (Wells et al. 1988). Given that morphotectonic features serve as significant indicators in evaluating relative tectonic activity (Bull et al. 1977; Keller et al. 1996; Burbank et al. 2001), we calculated six geomorphic indices: stream gradient index (SL), hypsometric integral (HI) (Strahler 1952) along with a hypsometric curve, drainage basin asymmetry (AF) (Hare et al. 1985), basin elongation ratio (Eb) (Schumm 1956), valley floor width to valley height ratio (Vf) (Bull et al. 1977), and transverse topography symmetry (T). These indices were correlated to evaluate tectonic activity in the study area. The methodology also integrates results from the analysis of the stream gradient index (*SL*) and validates these findings through field-based geomorphological observations. The effectiveness of such approaches has been demonstrated in other tectonically active regions, including the Shillong Plateau in northeast India (Mukteshwar 2019), the Central and Eastern Betic Cordillera in Spain (Azañón 2012), the Pacific coast of Costa Rica (Wells 1988), the southwestern USA (Rockwell et al. 1985), the Mediterranean Coast Spain (Cox 1994) the South-Western Sierra Nevada of Spain (Hamdouni et al. 2007) and the Kashmir Valley (Ahmad et al. 2012, 2013). This comprehensive analysis highlights the importance of morphotectonic features as indicators of tectonic activity and provides a reliable framework for evaluating tectonic processes.

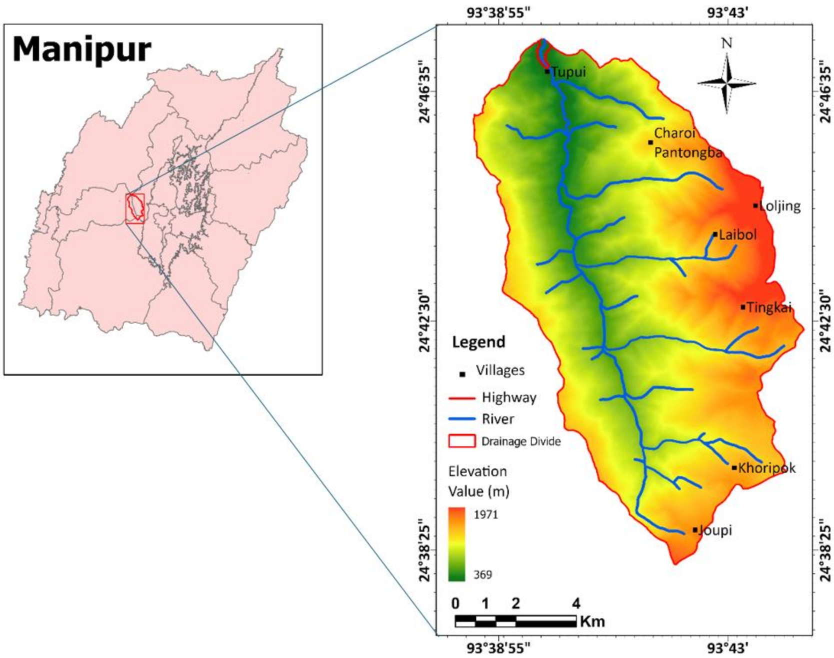

Fig. 1 Location map of the study area

The Tupul River watershed is located on the western side of the Imphal Valley, within the geographic coordinates of latitudes 24°47’32’’ to 24°37’54’’ N and longitudes 93°38’25’’ to 93°44’20’’ E. This study area falls within the Kangpokpi, Noney, and Churachandpur districts of Manipur state, India (Figure 1) covering a total catchment area of 101 km².

The drainage characteristics of this watershed is illustrated in Figure 2. The river originates from Laimaton in the Churachandpur District and extends up to Tupul in the Noney District, Manipur, where it converges with the Ijai River. The river generally flows in the direction of SSE to NNW, maintaining a perennial course of approximately 20.0 km. The basin predominantly exhibits a dendritic to trellis drainage pattern, reflecting the influence of underlying geological structures and topography.

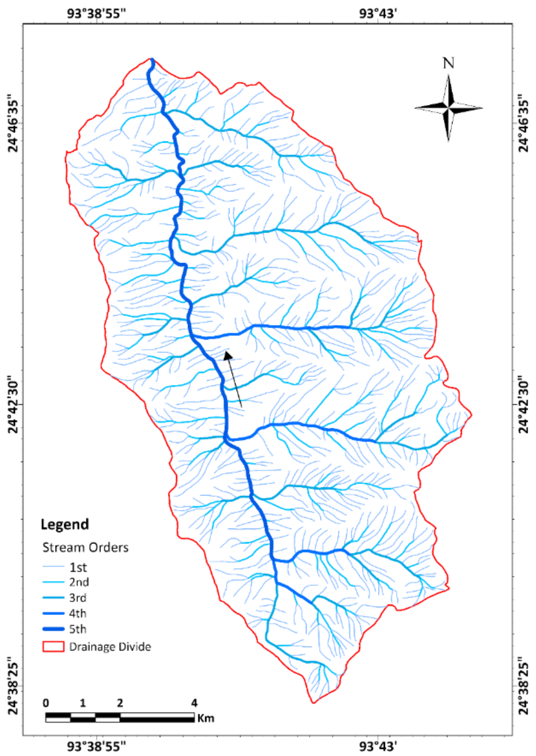

Fig. 2 Drainage characteristics of Tupul River basin

REGIONAL GEOLOGY AND TECTONIC SETUP

The geological formations of Manipur predominantly consist of Tertiary and Cretaceous sediments, with minor occurrences of igneous and metamorphic rocks. The Tertiary formations include sandstones, shales, siltstones, and mudstones, while the Cretaceous sediments comprise oceano-pelagic deposits such as chert and limestone. The Disang Group, dominating the study area and is characterized by thick splintery dark grey to black shales interbedded with siltstones and fine-grained sandstones. The term was first coined by Mallet in 1876. It is divided into the Lower Disang Formation, consisting mainly of dark grey to black coloured splintery shales, and the Upper Disang Formation, comprising intercalations of shales, siltstones and mudstones with minor amount of thinly bedded fine-grained sandstones.

Overlying the Disang Group is the Barail Group, which was first coined by Evans in 1932 to describe a thick sequence of arenaceous beds interbedded with shales. The Barail Group is subdivided into three formations: the Laisong Formation, consisting of alternating shales and fine- to medium-grained sandstones forming typical turbidite sequences; the Jenam Formation, dominated by carbonaceous shales with silt and sandstone bands; and the Renji Formation, which is characterized by massive to bedded sandstones. Geologically the study area is dominated by Disang group of rocks and in some parts of northeastern side Barail group of rocks are found (Figure 3).

The tectonic setting of Northeast India is shaped by active deformation due to compressive stress from Himalayan collision tectonics (Tapponnier et al. 1976). The study area serves as a transitional zone between the NE-SW trending Naga-Patkoi Hills and the N-S trending Mizoram and Chin Hills. Structurally, it is bounded by the Churachandpur-Mao Fault to the east and the Nungba Thrust to the west. The general lithological and tectonic trends are NNE-SSW, with variations to N-S, NE-SW, and occasionally NNW-SSE. The dip of the lithological units ranges from moderate to steep angles, typically towards the east or west.

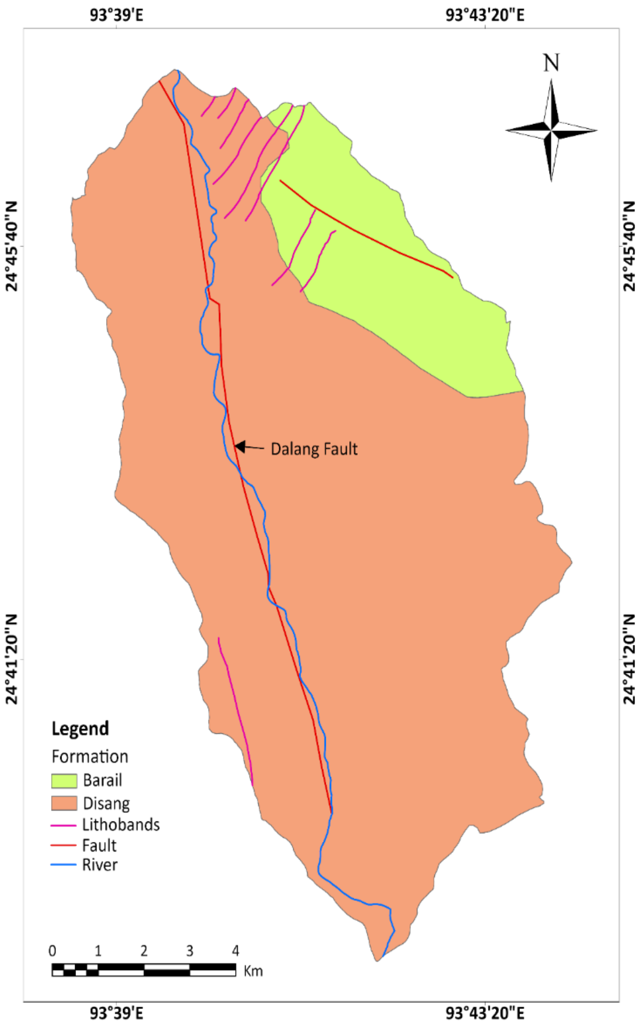

Fig. 3 Geological map of the study area (GSI 1992)

1 Seismotectonics

Manipur, one of the States of Northeast India, is in one of the most seismically active regions of the Indian subcontinent. It falls under Seismic Zone V, the highest category as per the Bureau of Indian Standards (IS 1893:2016), indicating a region of very high seismic hazard potential.

Manipur lies within the Indo-Burmese Arc, part of the Himalayan orogenic belt. Its seismicity is driven by the convergence of the Indian Plate with the Eurasian and Burmese Plates, active deformation along the Indo-Myanmar subduction zone, and a network of thrust, strike-slip faults, and folds. Key tectonic features include the Churachandpur-Mao Fault (a major N-S dextral strike-slip fault), the Kopili Fault (influential though located in Assam), and Myanmar's Sagaing Fault, capable of generating large earthquakes.

Table 1: Stratigraphic succession of the study area (Soibam 1998)

Litho-Unit and Age	Description of rocks	
Alluvium (Quaternary to Holocene)	Brownish to dark grey sand, silt, clay deposits with considerable amount of cobbles and gravels.	
------------------------------------ Stratigraphic break ------------------------------------		
Barail Group (Upper Eocene to Oligocene)	Renji Formation	Massive and Bedded Sandstone
	-------------------------- Gradational contact ----------------------	
	Jenam Formation	Intercalation of thinly bedded fine grained sandstone and shale
	-------------------------- Gradational contact ----------------------	
	Laisong Formation	Regressive sequence of shale, sandy shale and fine to medium grained sandstone with sedimentary structures like cross lamination, ripple marks etc.
------------------------------------ Gradational contact --------------------------------		
Disang Group	Upper Disang	Dark grey splintery shales intercalated with siltstone and fine grained sandstone. Shales are arenaceous and laminated.
	Lower Disang	Dark grey shales intercalated with mudstone and sandstone. Gritty sandstone, conglomerate, calcareous rocks.

The region has a history of moderate to high magnitude earthquakes, with accounts from local traditions and colonial records documenting destructive events in the 19^{th} and 20^{th} centuries. A notable recent event is the January 4, 2016, Mw 6.7 earthquake along the Tupul River, which caused significant damage and casualties in Imphal and in the study area. Ground motion was amplified by soft alluvial soils in the valley, with peak ground acceleration (PGA) reaching 0.2–0.35g in parts of the Imphal Valley. And also, GPS study of a regional dextral strike slip fault (Churachandpur-Mao-Fault, CMF) on the eastern side of the study area shows a motion of 16 mm/yr, and a fault normal motion of 8.7 mm/yr contributing to the upliftment (Gahalaut et al. 2013). This strong earthquake and the ongoing motion of the CMF shows active tectonic activities in the study area.

The b-value, a key indicator of regional earthquake recurrence and faulting behaviour, was analyzed for the Indo-Burma subduction zone in Northeast India. The region exhibits a heterogeneous b-value distribution ranging from 0.5 to 1.6, with an average of 0.96 (Bora et al. 2021). Lower b-values indicate compressive stress and high tectonic activity, especially along the Naga-Disang Thrust, Kabaw Fault, and Sagaing Fault, while higher b-values near the Indo-Burma Range (IBR) reflect tensional stress. The study reveals mixed faulting styles, dominated by thrust and strike-slip mechanisms. Depth analysis shows low b-values in the upper subducting slab due to higher stress, and unusually high b-values at greater depths, likely caused by slab weakening from dehydration. These findings offer crucial insights for seismic hazard assessment in the Indo-Burma region. And, also the regional recurrences, established based on past earthquake data, shows that the IBR is the most active block with the highest b value of 0.86±0.03 (Pallav et al. 2012).

2 Seismic Source Zones and Earthquake Potential

Several seismotectonic zones surround Manipur, which have potential for generating major earthquakes. Manipur's seismicity is governed by its location in a complex tectonic setting with active faults and subduction zones. The historical record, recent damaging events, and seismotectonic

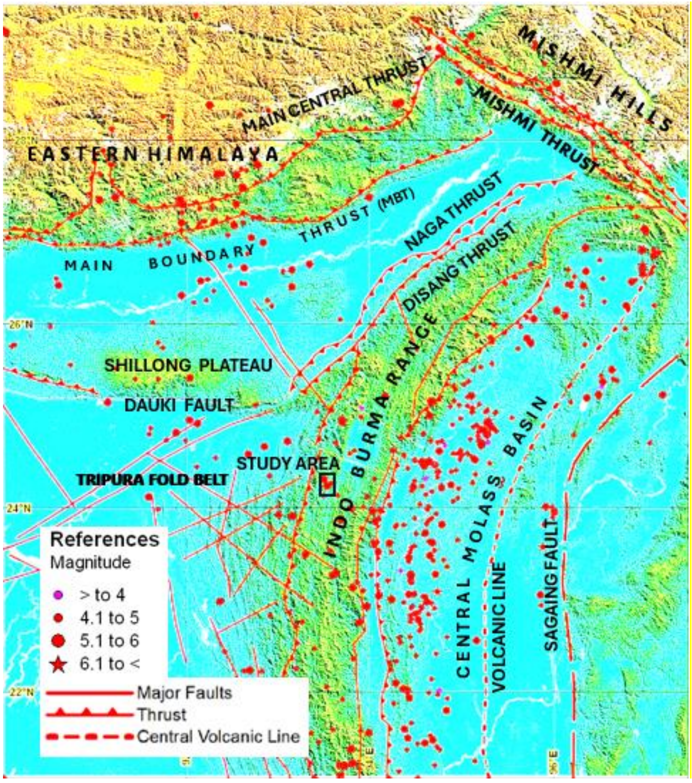

Fig. 4 Generalize seismotectonic map of NE-India and Indo-Myanmar region showing main regional structures

assessments emphasize the need for robust earthquake-resilient planning, detailed geotechnical investigations, and disaster preparedness strategies. Future development must integrate these risks into land-use planning, infrastructure design, and public safety measures.

The control region around the state is divided into seven tectonic zones to derive earthquake recurrence relations. Out of the seven zones, six (Eastern Himalaya, Mishmi Thrust, Naga Disang Thrust, Shillong Plateau, Bengal Basin and Assam Valley) are classified as shallow active and the IBR is classified as a subduction zone based on studies (Goswami et al. 1982; Nandy 2001).

Table 2: Seismic source with potential magnitudes

Seismic Source	Type	Potential Magnitude
Indo-Myanmar Subduction Zone	Subduction/Thrust	> 7.5
Churachandpur-Mao Fault	Strike-slip	6.5–7.0
Sagaing Fault (Myanmar)	Strike-slip	> 7.0
Local Reverse Faults	Thrust/Reverse	5.5–6.5

Frequent landslide events are very common in the vicinity of the Tupul river which follows the Dalang strike slip fault. As an example the massive landslide of 30th June 2022 near the under construction Tupul railway station with reported dead toll of 61 persons, believed to be triggered due to excessive rainfall of approximately 400% higher than the normal earlier recorded rainfall. And also, every year devastating landslides occurred along the NH-2 that runs near the regional fault CMF which is an active aseismic fault on the eastern side of the Tupul river (Gahalaut et al. 2013). The frequent occurring of major landslide emphasizes the need of assessment and studying the geology, tectonics, seismicity, stability of the slope and potential landslide triggering mechanisms.

MATERIAL AND METHODS

Survey of India toposheets at a scale of 1:50,000 (83H9 and 83G12), were utilized to delineate the study area and plan the execution of related works. For calculating geomorphic indices such as the stream gradient index (*SL*), valley floor width to valley height ratio (V_f), drainage basin asymmetry (*AF*), transverse topography symmetry (*T*), basin elongation ratio (E_b), hypsometric curve, and hypsometric integral, SENTINEL-2 satellite data and digital elevation models (DEM) were employed together with Global Mapper software (version 20.1), which significantly helped identifying tectonically active regions within the study area.

GEOMORPHIC INDICES AND RESULTS

1. Stream Gradient Index (*SL*)

The stream gradient index (*SL*) is an important tool for understanding the diastrophic forces and tectonic history of a region. It corresponds to changes in the stream's length relative to slope, lithology, or external loads, providing valuable insights into the area's geodynamic evolution. The *SL* index serves as a platform for evaluating how streams respond to tectonic processes, particularly uplift and displacement, which are often linked to active tectonics (Hack 1973; Keller et al. 1996; Burbank et al. 2001; Azor 2002; Chen et al. 2003; Pérez-Peña et al. 2009; Tsodoulos et al. 2008).

Rivers typically develop smooth concave longitudinal profiles, but variations in lithology or tectonic activity can cause fluctuations in the gradient, deviating from the ideal smooth shape. These fluctuations may reflect differences in rock resistance or indicate tectonic disturbance. Tectonically active rivers often exhibit a convex gradient profile at certain reaches, where abrupt changes in gradient are observed (Snow et al. 1987). High stream gradient (*SL*) values in areas with low or uniform rock resistance can serve as indicators of active tectonics (Keller 1986). As a result, changes in river profiles can be interpreted as responses to ongoing tectonic forces. The stream gradient index (*SL*) for a specific reach is defined by the equation below (Hack 1973). Figure 5 represents the idealised diagram for the calculation of *SL*.

$$SL = \frac{\Delta H}{\Delta L} . L$$

where, SL represents the stream gradient index, while $\Delta H / \Delta L$ denotes the channel slope or gradient of the reach and L refers to the total channel length from the specific point of interest where the index is being calculated, extending upstream to the highest point on the channel.

According to Hack (1973), the stream channel can be viewed as a connected series of segments, each with varying lengths, and these segments follow a logarithmic pattern. The stream gradient index (*SL*) is normalized by dividing each segment by *K* which is the graded river gradient of the stream and is defined as;

$$K = \frac{a - b}{lnL}$$

where, *a* is the elevation at source, *b* is the elevation at the mouth and *L* is the total stream length (Pérez-Peña et al. 2009; Yadava et al. 2022). The normalized stream gradient index for the segments is represented by *SL/K*.

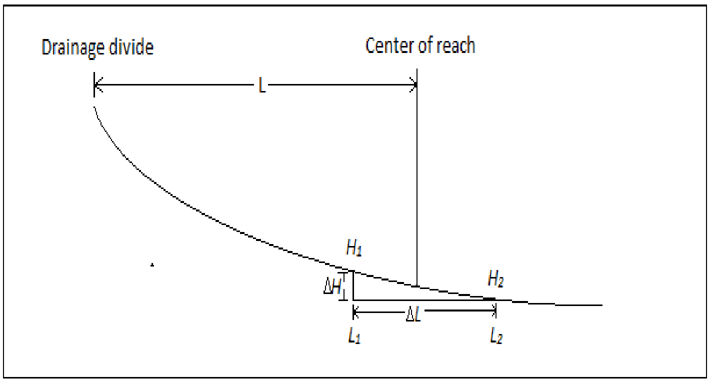

Fig. 5 A conceptual illustration depicting the calculation of SL for a specific reach (Hack 1973)

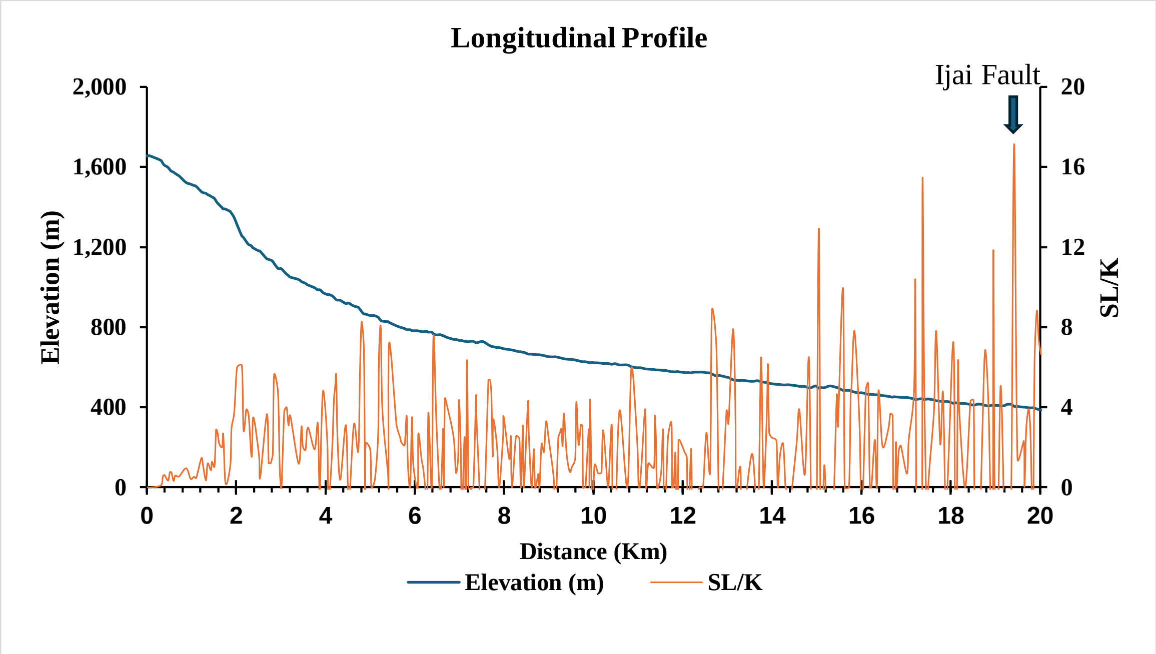

Fig. 6 Longitudinal profile along with *SL/K* of Tupul river

For the Tupul River, the calculated values of *SL/K* vary along the stresses of the river, with the maximum value of 17 where the mainstream intersects with the Ijai Fault (Figure 6). This increase in the *SL/K* value at the fault intersection may indicate tectonic influences on the river's gradient.

2 Valley Floor Width to Valley Height Ratio (V_f)

The ratio of valley floor width to valley height (V_f) serves as an indicator for assessing valley incision in elevated regions (Bull et al. 1977), and is defined as follows:

$$V_f = \frac{2V_{fw}}{(E_{ld} - E_{sc)} + (E_{rd} - E_{sc)}}$$

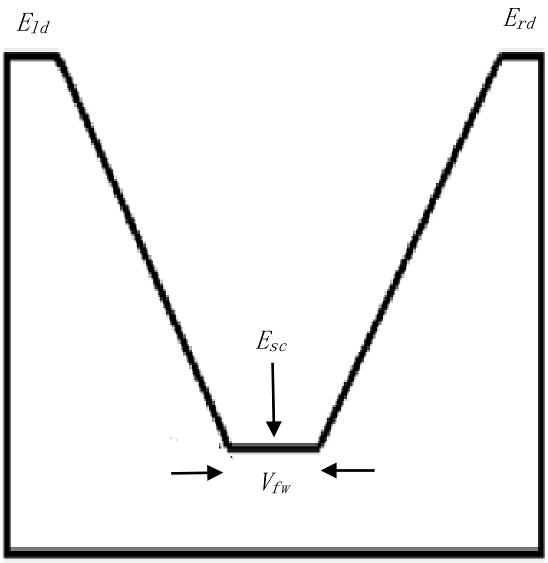

Fig. 7 An idealized diagram showing parameters for V_f calculation

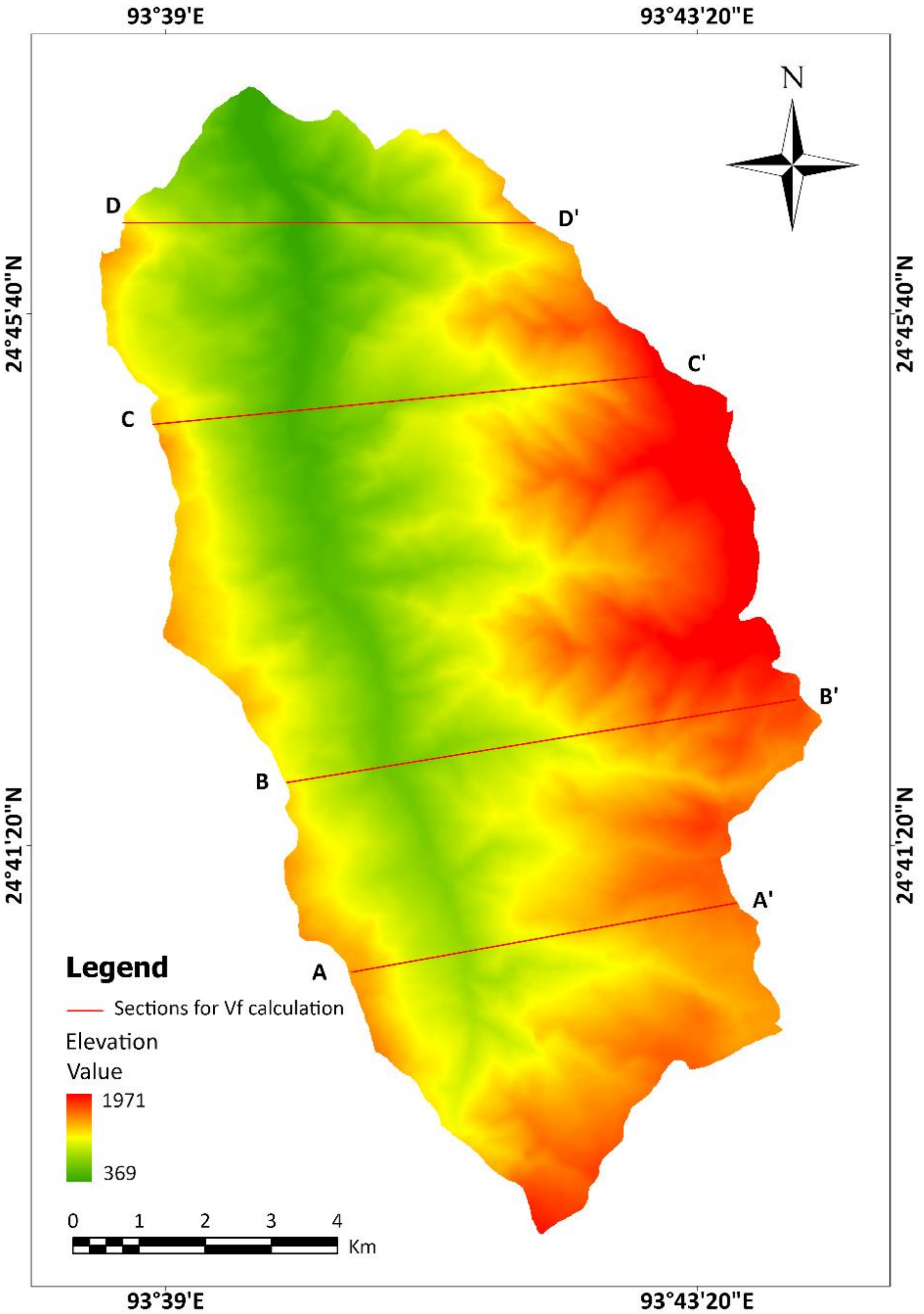

Fig.7a Location map from where the parameter V_f is calculated. AA', BB', CC' and DD' represent the sections to calculate the V_f

where, the valley floor width is denoted as V_{fw}, refers to the width of the valley for a specific profile at a fixed length. E_{rd} and E_{ld} represent the elevations of the right and left banks, respectively, for a given section line when facing downstream, while E_{sc} is the elevation of the valley floor (Figure 7).

V_f can be classified as V-shaped valleys with the values <1.0, where streams that are actively incising and are commonly associated with uplift; moderately active tectonics with the values between 1.0 and 1.5, and U-shaped valleys with the values >1.5 subjected to major lateral erosion (Bull et al. 1977).

The V_f values for the Tupul river basin have been calculated for four sections namely AA', BB', CC' and DD' (Figure 7a) and their profiles (Figure 7b). The calculated values range from 0.085 to 0.186 (Table 3). The V_f value of the study area suggests that the valley is V-shaped valley with streams that are actively incising and commonly associated with uplift. Therefore, the study area is tectonically active.

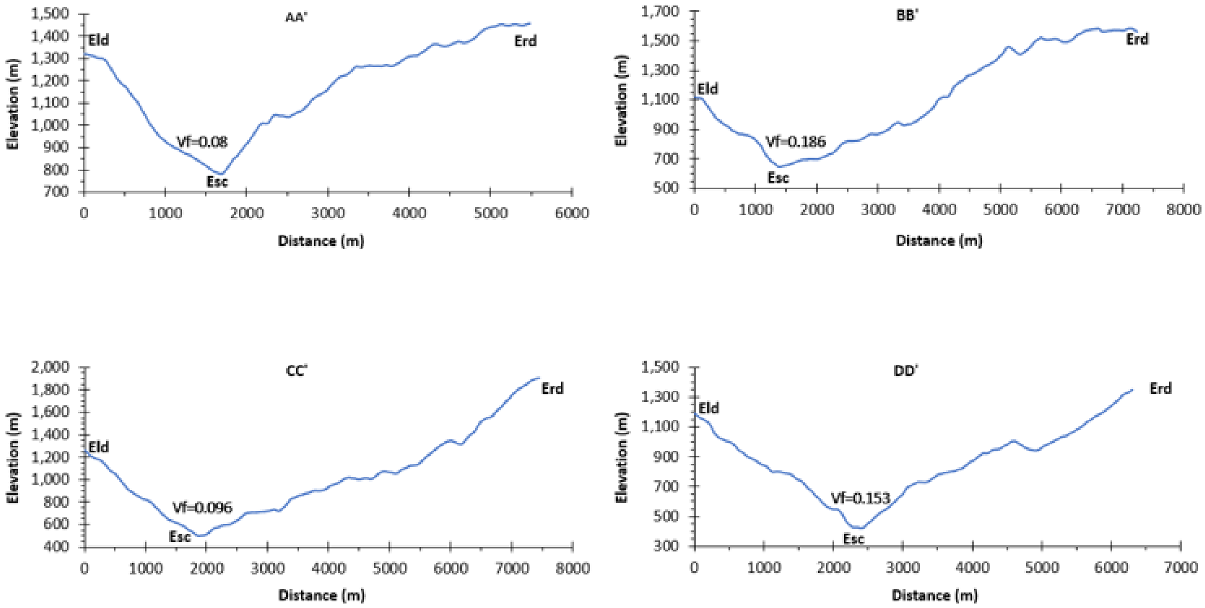

Fig. 7b Cross section profile for calculation of V_f. AA'(Eld-1323.26, Erd-1458.14, Esc-781.02, V_{fw}-52), BB'(Eld-1125.94, Erd-15262.73, Esc-644.45, V_{fw}-130), CC'(Eld-1271.34, Erd-1908.35, Esc-493.3, V_{fw}-105), DD'(Eld-1188.55, Erd-1349.28, Esc-418.02, V_{fw}-130)

3 Hypsometric Curve and Integral

The hypsometric curve is a key indicator of the geomorphic maturity of a basin, illustrating the distribution of elevation relative to the mean altitude of a catchment area (Strahler 1952). It serves as a valuable tool for differentiating between tectonically active and inactive regions (Keller et al. 1996). The shape of the hypsometric curve and the value of the hypsometric integral (H_i) provide insights not only into the erosional stage of the basin but also into the tectonic, climatic, and lithological factors that influence it (Moglen et al. 1995; Willgoose et al. 1998; Huang et al. 2006). High values of H_i indicate that most of the topography is relatively elevated, often in the form of upland surfaces with deeply incised streams, typically associated with youthful or active landforms. In contrast, intermediate and low H_i values suggest terrain subjected to extended erosion, resulting in more evenly dissected drainage basins, which are common in older landforms. Consequently, high H_i values are expected in regions with youthful landforms, while low values are indicative of more mature or old landscapes (Strahler 1952; Demoulin 1998; Keller et al. 2002). The formula for calculating the hypsometric integral is as follows (Pike et al. 1971):

$$H_i = \frac{H_{mean} - H_{min}}{H_{max} - H_{min}}$$

where, H_i is the hypsometric integral, H_{mean} is the mean elevation, and H_{min} and H_{max} are the lowest and highest elevations of the basin, respectively.

The necessary parameters for estimating the hypsometric integral (H_i), such as H_{min}, H_{max}, and H_{mean}, are derived through the application of ArcGIS's Raster Calculator and Zonal Statistics tools. The hypsometric curve for the Tupul River Basin is constructed by graphing the relative area (a/A) in relation to the relative height (h/H) (Figure 9). This formula defines "a" as the surface area within the basin above a designated elevation line, "A" as the total area of the basin, "h" as the elevation for which the calculation is conducted, and "H" as the highest elevation of the basin. Figure 8 presents the contour map detailing the calculation of h/H and a/A values for the 30-meter contour within the study area.

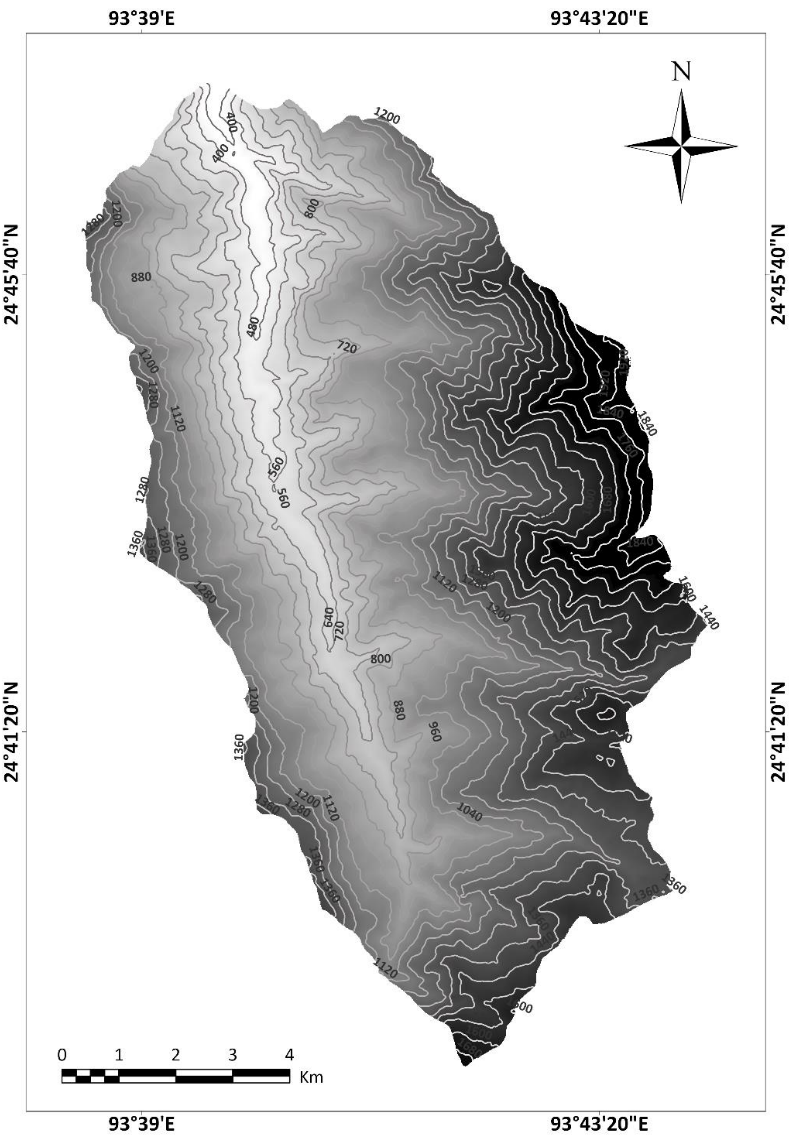

Fig. 8 Elevation Contour map for estimating a/A and h/H values

The computed H_i value for the watershed is 0.495, and the S-shaped curve depicted in Figure 9 indicates an early mature phase in the erosion cycle. This curve illustrates the tectonically active nature of the watershed, suggesting the region is probably undergoing continuous tectonic activities that influenced its geomorphological features.

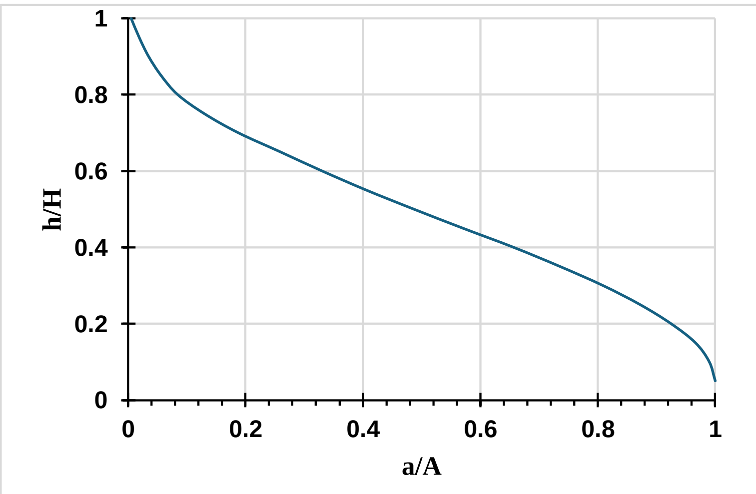

Fig. 9 Hypsometric curve of Tupul Basin

4 Drainage Basin Asymmetry (*AF*)

The Asymmetry Factor (*AF*) is a useful tool for assessing tectonic activity by analyzing the tilt of a river basin (Keller et al. 1996; Pérez-Peña et al. 2010). It helps to understand how the trunk stream of a drainage basin

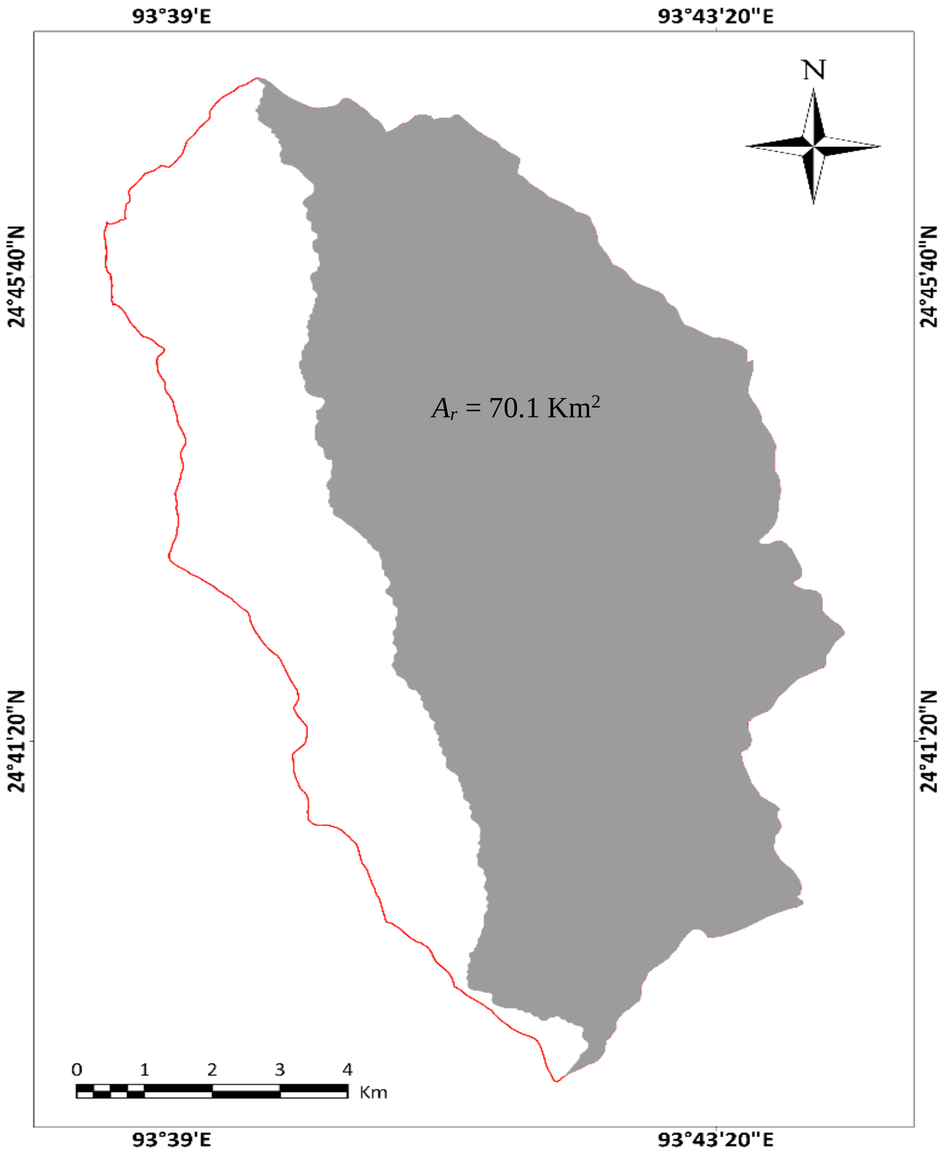

Fig. 10 Diagram representing A_r of the watershed

migrates in response to tectonic tilting (Morrish 2015). The tilting of the *AF* is typically perpendicular to the direction of the mainstream course, which aids in determining the tectonic influence on the river basin (Cox 1994; Tsodoulos et al. 2008). Drainage systems developed in regions undergoing tectonic deformation frequently display unique patterns and geometries.

The asymmetry factor, initially developed to identify the tectonic tilting characteristics of the basin (Hare et al. 1985), is defined as follows:

$$AF = 100.\frac{A_r}{A_t}$$

where, *AF* represents the asymmetry factor, while A_r denotes the area of the drainage basin located to the right side of the trunk channel when viewed from a downstream perspective. The total area of the drainage basin is represented by A_t. The *AF* must be set at 50% for a primary channel that has developed and persists in a consistent environment. The determination of tilt is influenced by whether *AF* is greater or less than 50% (Keller et al. 1996).

The calculated value of *AF* is shown in Table. 3 and its value is 70.32 % indicating that the channel has shifted downstream left side of the Tupul basin with an upliftment of North-eastern side.

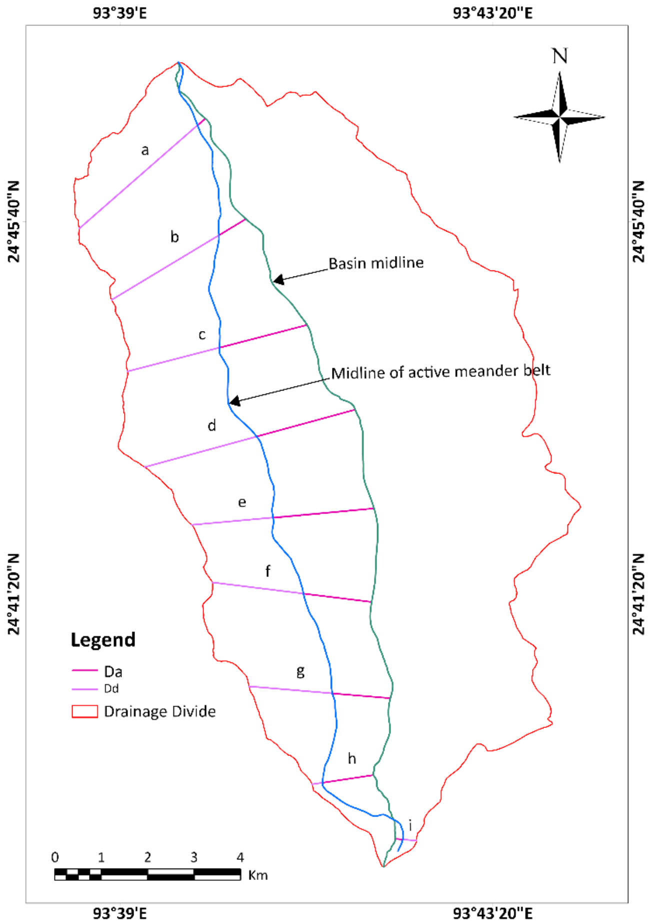

Fig. 11 Diagram representing the location map from where the value "*T*" is calculated. a-(Da-146.77, Dd-416.9), b-(Da-1007.47, Dd-1219.81), c-(Da-1142.67, Dd-2778.11), d-(Da-1347.52, Dd-3141.94), e-(Da-1989.08, Dd-3590.41), f-(Da-2014.41, Dd-4301.69), g-(Da-1788.51, Dd-3653.37), h-(Da-633.77, Dd-3150.4) and i-(Da-217.12, Dd-3424.69).

5 Transverse Topography Symmetry (*T*)

The Transverse Topographic Symmetry (*T*) is a quantitative parameter that describes the asymmetry of a river basin in both direction and magnitude (Keller et al. 1996). This index provides a numerical value, which indicates the degree of asymmetry in the basin, and an orientation, which shows the direction of that asymmetry (Pinter 2005). The transverse topographic symmetry is particularly useful for determining the tilt direction of a river and the magnitude of tectonic influences on the landscape (Cox 1994). If the value of this factor is greater than zero, it suggests that the river basin is asymmetric, which is often indicative of active tectonic forces affecting the region's topography (Keller et al.1996).

This factor is calculated by the equation which is given below

$$T = \frac{D_a}{D_d}$$

where, T represents the transverse topographic symmetry, D_a denotes the distance from the midline of the drainage basin to the midline of the active meander belt, and D_d indicates the distance from the midline of the basin to the drainage divide (Figure 11). Cox (1994) states that in a perfectly symmetric basin where T = 0, an increase in asymmetry leads T to approach the value of 1.

The traverse topography symmetry (*T*) for the watershed has been calculated along nine sections (Figure 11). The calculated values are 0.352, 0.826, 0.411, 0.429, 0.554, 0.468, 0.490, 0.201 and 0.063 for location a, b, c, d, e, f, g, h and i respectively. The average value is 0.422, almost approaching 1.0 and is asymmetric according to the Cox (1994). Therefore, the *T* values for the watershed show asymmetric in nature. which could be a result of active tectonic processes influencing the landscape.

6 Basin Elongation Ratio (E_b)

The Basin Elongation Ratio (E_b) is a quantitative morphometric parameter that reflects the shape of a river basin and provides valuable information about tectonic activity in the region (Bhattacharya et al. 2013). River basins undergoing active tectonism are typically elongated due to continuous thrusting and faulting (Burbank et al. 2001; Sreedevi et al. 2005; Argyriou et al. 2016). In contrast, a circular basin usually indicates an inactive geological setting, while an oval-shaped basin suggests a moderately active region (Bull et al. 1977). An elongated basin is often a sign of active tectonics (Bull et al. 1977). The Basin Elongation Ratio is calculated using an equation proposed by Schumm (1956), which compares the basin's area to its longest axis. This ratio helps to determine the level of tectonic activity in a basin, with more elongated shapes being associated with areas undergoing significant tectonic processes. Basin elongation ratio is defined as:

$$E_b = \frac{2\sqrt{A_b/\pi}}{l_b}$$

where, E_b is the elongation ratio, A_b is the area the basin, and l_b is the length of the basin measured from its mouth to most distant point on the watershed.

According to Chow (1964a), the Basin Elongation Ratio (E_b) typically ranges from 0.6 for elongate and tectonically active basins to 1.0 for tectonically quiescent, oval, and circular basins. Based on this classification, Chow (1964b) categorized drainage basins as circular (>0.9), oval (0.8-0.9), less elongate (0.7-0.8), and elongate (<0.7). Molin et al. (2004) observed that in landscapes experiencing active uplift,

Table 3: Calculated geomorphic indices of Tupul watershed

S. No.	Geomorphic indices	Value	Remarks
1	Basin Area (A)	101 km^2	Total basin area.
2	H_{max}	1971 m	Highest elevation
3	H_{min}	369 m	Lowest elevation
5	Hypsometric integral (H_i)	0.495	It shows youthful to mature basins.
6	Basin elongation ratio (E_b)	0.64	Reflects elongate basin and tectonically active.
7	Drainage basin asymmetry factor (AF)	70.32	Tilted basin in nature.
8	Transverse Topography Symmetry (T)	0.422	It shows asymmetric in nature.
9	Valley floor width to valley height ratio (V_f)	0.085 to 0.186	Indicates V-shaped valley with streams that are actively incising and commonly associated with uplifting.
10	Basin perimeter	47 km	

youthful basins are often relatively elongated. Bull and McFadden (1977) suggested that low values of the Basin Elongation Ratio are indicative of recent tectonic activity. For the Tupul River Basin, the calculated E_b value is 0.64, which is less than 0.7 (Table. 3), indicating an elongate shape. This result suggests that the Tupul River Basin is tectonically active in nature.

CONCLUSION

The analysis of various geomorphic indices, including the Stream Gradient Index, Valley Floor Width to Valley Height Ratio, Hypsometric Curve and Integral, Drainage Basin Asymmetry, Transverse Topography Symmetry, and Basin Elongation Ratio, leads to the conclusion that the Tupul River Basin is tectonically active. The study of the longitudinal profile with high *SL/K* values provides valuable insights into the morphotectonic nature of the watershed. The high Asymmetry Factor (AF = 70.32%) and the value of Transverse Topographic Symmetry (T = 0.422) indicate that the Tupul River watershed is undergoing tectonic tilting, with uplift on the right side (facing downstream). This has caused the river to shift laterally toward the left side of the valley. The Hypsometric Curve further supports the finding that the watershed is tectonically active. Additionally, the correlation of these parameters highlights the balance between erosional forces and tectonic forces, with tectonics dominating over erosion in shaping the landscape of the study area. The tectonically active nature of the study area is also supported by the presence of Dalang fault stretched along the Tupul river and Ijai fault are also one of the major reason of January 4th 2016 earthquake along the Tupul river with a magnitude of Mw 6.7. The ongoing activity of CMF resolved from the permanent and campaign GPS data also supports the active tectonic of the study area.

REFERENCES

1. Ahmad, S. and Bhat, M.I. (2012). "Tectonic Geomorphology of Rambiara Basin, SW Kashmir Valley Reveals Emergent Out-of-Sequence Active Fault System", *Himalayan Geology*, Vol. 33, No. 2, pp. 162-172.
2. Ahmad, S., Bhat, M.I., Madden, C. and Bali, B.S. (2013). "Geomorphic Analysis Reveals Active Tectonic Deformation on the Eastern Flank of the Pir Panjal Range, Kashmir Valley, India", *Arabian Journal of Geosciences*.
3. Argyriou, A.V. and Teeuw, R.M. (2016). "GIS Multi-Criteria Decision Analysis for Assessment and Mapping of Neotectonic Landscape Deformation: A Case Study from Crete", *Geomorphology*, Vol. 253, pp. 262-274.
4. Azañón, J.M., Pérez-Peña, J.V., Giaconia, F., Booth-Rea, G., Martínez-Martínez, J.M. and Rodríguez-Peces, M.J. (2012). "Active Tectonics in the Central and Eastern Betic Cordillera through Morphotectonic Analysis: the case of Sierra Nevada and Sierra Alhamilla", *Journal of Iberian Geology*, Vol. 38, No. 1, pp. 225–238.
5. Azor, A., Keller, E.A. and Yeats, R.S. (2002). "Geomorphic Indicators of Active Fold Growth: South Mountain-Oak Ridge Ventura basin, Southern California", *Geological Society of America, Bull.*, Vol. 114, pp. 745-753.
6. Bhattacharya, F., Rastogi, B.K. and Kothyari, G.C. (2013). "Morphometric Evidence of Seismicity around Wagad and Gedi Faults, Eastern Kachchh, Gujarat", *Journal of Geological Society of India*, Vol. 81, pp. 113-121.
7. Bora, D.K., Borah, K., Singh, A.P. and Mishra, O.P. (2021). "Distribution of B-Values in Indo-Burma Ranges, Northeast India: Implications to Structural heterogeneities and Style of Faulting", *Geological Journal*, Vol. 57, No. 12, pp. 5284-5293. https://doi.org/10.1002/gj.4294.
8. Bull, W.B. and McFadden, L.D. (1977). "Tectonic Geomorphology North and South of the Garlock Fault, California", *In: Doehring, D.o., Ed., Geomorphology in Arid Regions, Proceedings 8th Annual Geomorphology Symposium, State University, of New York, Binghamton*, pp. 115-138.
9. Burbank, D. and Anderson, R. (2001). "Tectonic Geomorphology", *Blackwell Science, Oxford*.
10. Chen, Y.C., Sung, Q. and Cheng, K.Y. (2003). "Along-Strike Variations of Morphotectonic Features in the Western Foothills of Taiwan: Tectonic Implications Based on Stream — Gradient and Hypsometric Analysis", *Geomorphology*, Vol. 56, No. 1, pp. 109-137.
11. Chow, V.T. (1964a). "Handbook of Applied Hydrology: A Compendium of Water Resources Technology", *McGraw Hill, New York*, pp. 4-11.
12. Chow, V.T. (1964b). "Handbook of Applied Hydrology: A Compendium of Water Resources Technology", *McGraw Hill, New York*, pp.7-10.
13. Cox, R.T. (1994). "Analysis of Drainage Basin Symmetry as a Rapid Technique to Identify Areas of Possible Quaternary Tilt-Block Tectonics: An Example from the Mississippi Embayment", *Geological Society of America, Bull.*, Vol. 106, pp. 571-581.
14. Demoulin, A. (1998). "Testing the Tectonic Significance of some Parameters of Longitudinal River Profiles: The Case of the Ardenne (Belgium, NW Europe)", *Geomorphology*, Vol. 24, No. 2-3, pp. 189-208.
15. El Hamdouni, R., Irigaray, C., Fernandez, T., Chacón, J. and Keller, E.A. (2007). "Assessment of Relative Active Tectonics, Southwest Border of Sierra Nevada (Southern Spain)", *Geomorphology*, Vol. 96, pp. 150–173.
16. Evans, P. (1932). "Tertiary Succession of Assam", *Transactions of the Mining and Geological Institute of India*, Vol. 27, No. 23, pp. 155-260.

17. Gahalaut, V.K., Kundu, B., Laisharm, S.S., Catherine, J., Kumar, A., Singh, M.D., Tiwari, R.P., Chadha, R.K., Samanta, S.K., Ambikapathy, A., Mahesh, P., Amit Bansal and Narsaiah, M. (2013). "Aseismic plate boundary in the Indo-Burmese Wedge", *Northeast Sunda Arc, Geology*, Vol. 41, No. 2, pp. 235-238.
18. Geological Survey of India (1992). "Geology and Structure of the Areas around Tupul, Kharam, Houchong, Ponlen and Kabuikhul, Tamenglong" *District, Manipur, (For restricted circulation)*.
19. Goswami, H. C. and Sarmah, S. K. (1982). "Probabilistic Earthquake Expectancy in the Northeast Indian Region Bull.", *Seismol. Soc. Am.*, Vol. 72, pp. 999–1009.
20. Hack, J.T. (1973). "Stream-Profile Analysis and Stream Gradient Index", *Journal Research of United State Geological Survey*, Vol. 1, pp. 1421-1429.
21. Hare, P.H. and Gardner, T.W. (1985). "Geomorphic Indicators of Vertical Neotectonism along Converging Plate Margins, Nicoya Peninsula, Costa Rica", *In: Morisawa, M., Hack, J.T. (Eds.), Tectonic Geomorphology. Allen and Unwin, Boston*, pp. 75-104.
22. Huang, X.J. and Niemann, J.D. (2006). "Modelling the Potential Impacts of Groundwater Hydrology on Long-Term Drainage Basin Evolution", *Earth Surface Processes and Landforms*, Vol. 31, pp. 1802-1823.
23. Keller, E.A. (1986). "Investigation of Active Tectonics: Use of Surficial Earth Processes. In: Wallace, R.E. (Ed.), Active Tectonics. Studies in Geophysics", *National Academy Press, Washington DC*, pp.136-147.
24. Keller, E.A. and Pinter, N. (1996). "Active Tectonics: Earthquakes Uplift and Landscapes", *2nd Prentice Hall, New Jersey*, pp. 338
25. Keller, E.A. and Pinter, N. (2002). Active Tectonics: Earthquakes, Uplift, and Landscape", *second ed. Englewood Cliffs, New Jersey, Prentice Hall*, pp. 362.
26. Mallet, F.R. (1876). "On the Coal Fields of Naga Hills Bordering Lakhimpur and Sibsagar Districts, Assam", *Memoirs of the Geological Survey of India*, Vol. 12, No. 2, pp. 286.
27. Moglen, G.E. and Bras, R.L. (1995). The Effect of Spatial Heterogeneities on Geomorphic Expression in a Model of Basin Evolution", *Water Resources Research*, Vol. 31, pp. 2613-2623.
28. Molin, P., Pazzaglia, F.J. and Dramis, F. (2004). "Geomorphic Expression of Active Tectonics in a Rapidly-Deforming Forearc, Sila Massif, Calabria, Southern Italy", *American Journal of Science*, Vol. 304, No. 7, pp. 559-589.
29. Morrish, S.C. (2015). "Characterization and Digital Morphotectonic Analysis of Drainage Basins in a Deforming Forearc, Nicoya Peninsula", *Thesis: California State Polytechnic University, Pomona*.
30. Mukteshwar, N.M. (2019). "Active Tectonic Deformation of the Shillong Plateau, India: Inferences from River Profiles and Stream-Gradients", *Journal of Asian Earth Sciences*, Vol. 181, pp. 1-23.
31. Nandy, D. R. (2001). "Geodynamics of Northeastern India and the Adjoining Region", *(Kolkata: ABC Publications)*.
32. Pallav, K., Raghukanth, S.T.G., and Singh, K.D. (2012). "Probabilistic Seismic Hazard Estimation of Manipur, India", *Journal of Geophysics and Engineering*, Vol. 9, No. 5, pp. 516–533. https://doi.org/10.1088/1742-2132/9/5/516.
33. Pérez-Peña, J.V., Azañón, J.M., Azor, A., Delgado, J. and González- Lodeiro, F. (2009). "Spatial Analysis of Stream Power Using GIS: SL Anomaly Maps", *Earth Surface Processes and Landforms*, Vol. 34, pp. 16-25.
34. Pérez-Peña, J.V., Azor, A., Azañón, J.M. and Keller, E.A. (2010). "Active Tectonics in the Sierra Nevada (Betic Cordillera, SE Spain): Insights from Geomorphic Indexes and Drainage Pattern Analysis", *Geomorphology*, Vol. 119, pp. 74-87.
35. Pike, R.J. and Wilson, S.E. (1971). "Elevation-Relief Ratio, Hypsometric Integral and Geomorphic Area-Altitude Analysis", *Geological Society of America, Bull*., Vol. 62, pp. 1079-1084.
36. Pinter, N. (2005). "Applications of Tectonic Geomorphology for Deciphering Active Deformation in the Pannonian Basin, Hungary", *Occasional Papers of the Geological Institute of Hungary*, Vol. 204, pp 25-51.
37. Rockwell, T.K., Keller, E.A. and Johnson, D.L. (1985). "Tectonic Geomorphology of Alluvial Fans Sand Mountain Front near Ventura, California", *In: Morisawa, M., Hack, J.T. (Eds.), Tectonic*

Geomorphology –Proceedings of the 15th Annual Binghampton Geomorph. Symp. Sep. 1984. Allen and Unwin, pp. 183-208.

38. Schumm, S.A. (1956). "Evolution of Drainage Systems and Slopes in Badlands at Perth Amboy, New Jersey", *Geological Society of America, Bull.*, Vol. 67, pp. 597-646.
39. Snow, R.S. and Slingerland, R.L. (1987). "Mathematical Modeling of Graded River Profiles", *The Journal of Geology*, Vol. 95, pp. 15-33.
40. Soibam, I. (1998). "Structural and Tectonic analysis of Manipur with special reference to evolution of the Imphal Valley", Unpublished Ph.D. Thesis, Manipur University Imphal.
41. Sreedevi, P.D., Subrahmanyam, K. and Shakeel, A. (2005). "The Significance of Morphometric Analysis for Obtaining Groundwater Potential Zones in a Structurally Controlled Terrain", *Environmental Geology*, Vol. 47, No. 3, pp. 412-420.
42. Strahler, A. (1952). "Dynamic Basis of Geomorphology", *Geological Society of America, Bull.*, Vol. 63, No. 9, pp. 923 938.
43. Tapponnier, P. and Molnar, P. (1976). "Slip Line Field Theory and Large-Scale Continental Tectonics", *Nature*, Vol. 264, No. 5584, pp. 319-324.
44. Tsodoulos, I.M., Koukouvelas, I.K. and Pavlides, S. (2008). "Tectonic Geomorphology of the Easternmost Extension of the Gulf of Corinth (Beotia, Central Greece)", *Tectonophysics*, Vol. 453, No. 1, pp. 211-232.
45. Wells, S.G., Bullard, T.F., Menges, T.M., Drake, P.G., Karas, P.A., Kelson, K.I., Ritter, J.B. and Wesling, J.R. (1988). "Regional Variations in Tectonic Geomorphology along Segmented Convergent Plate Boundary, Pacific Coast of Costa Rica", *Geomorphology*, Vol. 1, pp. 239-265.
46. Willgoose, G. and Hancock, G. (1998). "Revisiting the Hypsometric Curve as an Indicator of Form and Process in Transport Limited Catchment", *Earth Surface Processes and Landforms*, Vol. 23, pp. 611-623.
47. Yadava, S.K. and Singh, S.K. (2022). "Morpho-Tectonic Assessment of Central Northern Escarpment of Peninsular India, Based on Tectonically Sensitive Geomorphic Indices", *Physical Geography*, Vol. 43, No. 6, pp. 753-783.